

Development and Verification of Liquid-Fueled Molten Salt Reactor Analysis Code Based on RELAP5

Chengbin Shi, Maosong Cheng and Guimin Liu

Abstract Liquid-fueled molten salt reactor is the only reactor system using liquid salt as fuel in the six generation IV advanced reactor systems, which can be characterized by remarkable advantages and competitiveness in nuclear safety, economical efficiency, natural resource protection, sustainable development, and proliferation resistance of nuclear energy. Each country in the world is carrying out research on the molten salt reactor, and system analysis is an important research content. RELAP5 code is the best estimation code of pressurized water reactor. In this paper the neutronics and thermal hydraulics models in the RELAP5 are extended, so as to develop a system analysis code for liquid-fueled molten salt reactor. Then the code is verified using molten salt reactor experiment (MSRE) experimental benchmarks. The results indicate that the computational results coincide well with MSRE experimental benchmarks, and preliminary verifies the validity of the extended system analysis code.

Keywords RELAP5 · Liquid-fueled molten salt reactor · MSRE · Code verification

1 Introduction

The molten salt reactor (MSR) is one of the six advanced reactor concepts identified by the Generation IV International Forum (GIF) as a candidate for cooperative development. The study on the molten salt reactors was first carried out at the Oak Ridge National Laboratory (ORNL) in the projects of the Aircraft Reactor Experiment (ARE) [1] and the Molten Salt Reactor Experiment (MSRE) [2]. Based on the experience of running MSRE, ORNL then published the Molten Salt Breeder Reactor (MSBR) conceptual design [3]. The research of MSR in Japan started from

C. Shi · M. Cheng (✉) · G. Liu
Shanghai Institute of Applied Physics, Chinese Academy of Sciences,
Shanghai 201800, China
e-mail: chengmaosong@sinap.ac.cn

1980s, and the FUJI concept was published referred to the MSBR design [4]. Besides, in Russia, a new molten salt reactor concept, named the Molten Salt Actinide Recycler and Transmuter (MOSART), has been developed for burning transuranium plutonium and minor actinides [5]. In January 2011, Chinese Academy of Science launched a strategic pilot science and technology special project “Thorium Molten Salt Reactor Nuclear Energy System (TMSR),” aiming at developing both solid and liquid-fueled molten salt reactors [6].

Up to now, the characteristics of molten salt reactor have been studied by different researchers with various computational codes. The Cinsf1D code in one-dimension geometry using two-energy-group diffusion and a spatial dimension neutronic model was developed by Lecarpentier and Carpentier [7]. Krepel et al. [8, 9] extended the DYN1D/DYN3D code for liquid-fueled molten salt reactors, in which the neutron diffusion models were employed for neutrons calculation. Wang et al. [10] analyzed the fluid dynamic of the MOSART core with the code SIMMER-III by extending the thermo hydraulic and neutronic models. Guo et al. [11] developed the safety analysis code by considering the delayed neutron precursors both in the reactor core and the external loop.

The RELAP5 code is the thermal hydraulic best estimate code for pressurized water reactor, which was originally developed by Nuclear Regulatory Commission (NRC). In this work, the point kinetic model including the flow effect of liquid-fueled molten salt reactor and the thermal hydraulic model with internal heat source were embedded into the RELAP5 code. Then the dynamics of the MSRE were simulated to verify the validity of the extended RELAP5 code.

2 Physical Models and Solution Methods

2.1 Neutronics Model

According to the conservation law, the neutron equation of the reactor core can be written as

$$\frac{dn(t)}{dt} = \frac{\rho(t) - \beta_{\text{eff}}}{l} n(t) + \sum_{i=1}^6 \lambda_i c_i(t), \quad (1)$$

where n is the neutron density; ρ is the reactivity; β_{eff} is the portion of effective delayed neutron precursors; l is the neutron lifetime. Delayed neutron precursors in the liquid-fueled molten salt reactor flow with the liquid fuel in the primary loop, which is different from the traditional solid fueled reactor. Considering that delayed neutron precursors decay in the primary loop and flow back into the reactor core again, the delayed neutron conservation equation can be expressed as

$$\frac{dc_i(t)}{dt} = \frac{\beta_i}{l} n(t) - \left(\lambda_i + \frac{1}{\tau_c} \right) c_i(t) + \frac{\exp(-\lambda_i \tau_l)}{\tau_c} c_i(t - \tau_l), \quad (2)$$

where β_i is the portion of neutron fraction of group i ; τ_c is the time of delayed neutron precursors staying in the core; τ_l is the time of delayed neutron precursors staying in the external loop. The second term in the right side of Eq. (2) indicates the reduced delayed neutron precursors due to the decay and flow effect of fuel salt, and the third term in right side of Eq. (2) indicates the delayed neutron precursors flow back into the core. From Eqs. (1) and (2), the reactivity bias $\Delta\rho_0$ can be obtained by setting the left side of the above equations to zero. The reactivity bias due to the liquid fuel flow in steady state can be expressed as

$$\Delta\rho_0 = \sum_{i=1}^6 \beta_i \left[1 - \frac{\lambda_i}{\lambda_i + \frac{1}{\tau_c} (1 - \exp(-\tau_l \lambda_i))} \right] \quad (3)$$

Reactivity feedback can be induced by temperature change, void fraction, power change. However, in this work, only reactivity feedback due to temperature change of fuel and graphite is taken into account. Therefore, reactivity feedback can be expressed as

$$\rho(t) = \Delta\rho + \rho_{\text{fuel}} + \rho_{\text{graphite}} \quad (4)$$

$$\rho_{\text{fuel}} = \alpha_{\text{fuel}} (T_{\text{fuel}} - T_{0,\text{fuel}}) \quad (5)$$

$$\rho_{\text{graphite}} = \alpha_{\text{graphite}} (T_{\text{graphite}} - T_{0,\text{graphite}}), \quad (6)$$

where ρ_{fuel} is the reactivity feedback of fuel salt in reactor core; ρ_{graphite} is the reactivity feedback of graphite in reactor core; T_{fuel} is the average temperature of fuel salt in reactor core; $T_{0,\text{fuel}}$ is the initial temperature of fuel salt in reactor core; T_{graphite} is the average temperature of fuel salt in reactor core; $T_{0,\text{graphite}}$ is the initial temperature of fuel salt in reactor core; α_{fuel} is the feedback coefficient of fuel salt; α_{graphite} is the feedback coefficient of graphite.

2.2 Thermal Hydraulic Model

For single-phase molten salt, liquid and vapor phase conservation equation need to be calculated, respectively, while vapor phase fraction sets to be a minimal value in the RELAP5.

Two-phase mass conservation equation can be written as following:

$$\frac{\partial}{\partial t} (\alpha_g \rho_g) + \frac{1}{A} \frac{\partial}{\partial x} (\alpha_g \rho_g v_g A) = \Gamma_g \quad (7)$$

$$\frac{\partial}{\partial t} (\alpha_f \rho_f) + \frac{1}{A} \frac{\partial}{\partial x} (\alpha_f \rho_f v_f A) = \Gamma_f, \quad (8)$$

where α is the fraction of fluid, ρ represents the density, v is the speed of fluid flow, the subscript f and g represent the liquid and the vapor phase, respectively, the terms in the right side of Eqs. (7) and (8) indicate the generation rate of vapor Γ_g and liquid Γ_f . The overall continuity consideration requires that the liquid generation term needs to be the negative to the vapor generation.

Based on the assumption that the Reynolds stresses, the universally covariance terms, interfacial momentum storage, and phasic viscous stresses are neglected, the phasic pressures are assumed equal, the interfacial pressure is assumed equal to the phasic pressures, the interface force terms consist of both pressure and viscous stresses, and the normal wall forces are assumed adequately modeled by the variable area momentum flux formulation, two-phase momentum conservation equations can be written as following:

$$\begin{aligned} \alpha_g \rho_g A \frac{\partial v_g}{\partial t} + \frac{1}{2} \alpha_g \rho_g A \frac{\partial v_g^2}{\partial x} &= -\alpha_g A \frac{\partial P}{\partial x} + \alpha_g \rho_g B_x A - (\alpha_g \rho_g A) \text{FWG}(v_g) \\ &+ \Gamma_g A (v_{gl} - v_g) - (\alpha_g \rho_g A) \text{FIG}(v_g - v_f) \\ &- C \alpha_g \alpha_f \rho_m A \left[\frac{\partial (v_g - v_f)}{\partial t} + v_f \frac{\partial v_g}{\partial x} - v_g \frac{\partial v_f}{\partial x} \right] \end{aligned} \quad (9)$$

$$\begin{aligned} \alpha_f \rho_f A \frac{\partial v_f}{\partial t} + \frac{1}{2} \alpha_f \rho_f A \frac{\partial v_f^2}{\partial x} &= -\alpha_f A \frac{\partial P}{\partial x} + \alpha_f \rho_f B_x A - (\alpha_f \rho_f A) \text{FWG}(v_f) \\ &- \Gamma_g A (v_{fl} - v_f) - (\alpha_f \rho_f A) \text{FIG}(v_f - v_g) \\ &- C \alpha_f \alpha_g \rho_m A \left[\frac{\partial (v_f - v_g)}{\partial t} + v_g \frac{\partial v_f}{\partial x} - v_f \frac{\partial v_g}{\partial x} \right], \end{aligned} \quad (10)$$

where P is the pressure, B_x is the acceleration of body force, FWG is the wall friction drag coefficient, FIG is the interface friction drag coefficient, the terms in the right side of Eqs. (9) and (10) denote the pressure gradient, the body force, wall friction drag, momentum transfer due to interface mass transfer, interface frictional drag, and force due to virtual mass, respectively.

With the simplification of neglecting the Reynolds heat flux, the universally covariance terms, the interfacial energy storage, and internal phasic heat transfer, two-phase energy conservation equations can be written as following:

$$\begin{aligned} \frac{\partial}{\partial t} (\alpha_g \rho_g U_g) + \frac{1}{A} \frac{\partial}{\partial x} (\alpha_g \rho_g U_g v_g A) &= -P \frac{\partial \alpha_g}{\partial t} - \frac{P}{A} \frac{\partial}{\partial x} (\alpha_g v_g A) + Q_{wg} + Q_{ig} \\ &+ \Gamma_{ig} h_g^* + \Gamma_w h_g' - Q_{gf} + \text{DISS}_g + S_g \end{aligned} \quad (11)$$

$$\frac{\partial}{\partial t}(\alpha_f \rho_f U_f) + \frac{1}{A} \frac{\partial}{\partial x}(\alpha_f \rho_f U_f v_f A) = -P \frac{\partial \alpha_f}{\partial t} - \frac{P}{A} \frac{\partial}{\partial x}(\alpha_f v_f A) + Q_{wf} + Q_{if} - \Gamma_{ig} h_f^* - \Gamma_w h_f' + Q_{gf} + \text{DISS}_f + S_f, \quad (12)$$

where the Q is the heat transfer rate, h is the phasic enthalpy, DISS is the dissipation term, and S is the source term. Due to the fluid salt acting as both fuel and coolant, this paper add new internal heat source terms (S_g and S_f) based on the original energy conservation equations, and create new control volume with internal heat source in RELAP5 code.

2.3 Solution Methods

The thermal hydraulics and the neutronics models are solved separately in RELAP5 code, where the solution of the thermal hydraulic model adopts semi-implicit method for pressure–velocity linked equations. Noticing that the third term in the right side of Eq. (2) contains the retarded term, this equation belongs to the delay differential equation, which can be solved by a special fifth-order Runge–Kutta method [12, 13].

The coupling process of thermal hydraulic module and point kinetic module in RELAP5 code is shown in Fig. 1. The thermal hydraulic module gets the reactor power data calculated by point kinetic model, and then carries out flow and heat transfer calculation, which works out the temperature and density of coolant and moderator of each segment. The point kinetic module gets the temperature and density data of coolant and moderator calculated by thermal hydraulic model, and processes feedback calculation. Thus, reactor power can be calculated from neutron flux.

3 Code Verification

In June 1965, the Oak Ridge National Laboratory processed the zero power reactor physics experiment of MSRE, and tested the response of reactivity to flow rate in fuel pump start-up and coast-down transients with the reactor critical [14]. In the late running period of MSRE, ORNL carried on the nature circulation experiment with the U-233 fuel, which made sure the residual heat removal character of MSRE primary system [15].

This paper verifies the expanded code using the MSRE fuel pump start-up, fuel pump coast-down and natural circulation experiment data. MSRE data using in verification is listed in Tables 1 and 2.

The comparison of calculation result and experiment data of fuel pump start-up and coast-down transient is shown in Fig. 2. As the fuel pump starts up, a portion of

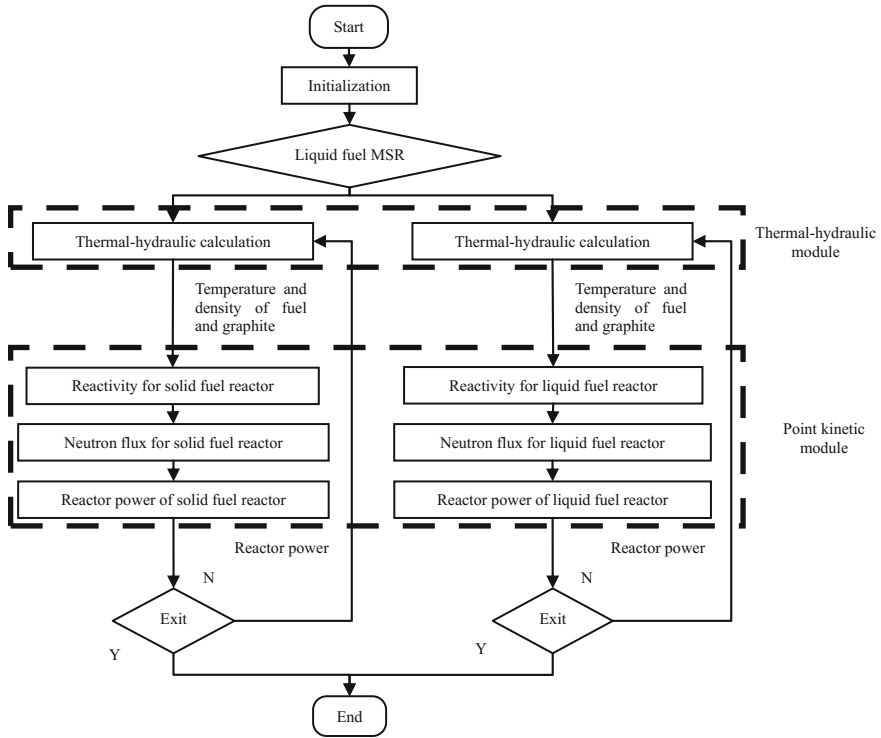


Fig. 1 Flow chart of the point kinetic module coupling with the thermal hydraulic module

Table 1 MSRE parameter [16, 17]

Parameter	U-235	U-233
Reactivity coefficient of fuel salt $\alpha_{\text{fuel}}/(\text{pcm/K})$	-8.46	-9.54
Reactivity of graphite $\alpha_{\text{graphite}}/(\text{pcm/K})$	-4.68	-5.76
Neutron lifetime l/s	0.000240	0.00040
Effective delayed neutron fraction β_{eff}	0.006661	0.002894
Fuel salt density $\rho_{\text{fuel}}/(\text{kg/m}^3)$	2263.0	2263.0
Specific heat of fuel salt $c_{p_fuel}/(\text{J}/(\text{kg K}))$	1982.5	1982.5

Table 2 Delayed neutron data in MSRE [17]

Group	U-235		U-233	
	λ/s^{-1}	$\beta_{\text{eff}}/10^{-5}$	λ/s^{-1}	$\beta_{\text{eff}}/10^{-5}$
1	0.0124	22.3	0.0126	23.76
2	0.0305	145.7	0.0337	85.76
3	0.111	130.7	0.139	71.90
4	0.301	262.8	0.325	82.14
5	1.14	76.6	1.13	15.79
6	3.01	28	2.5	10.03

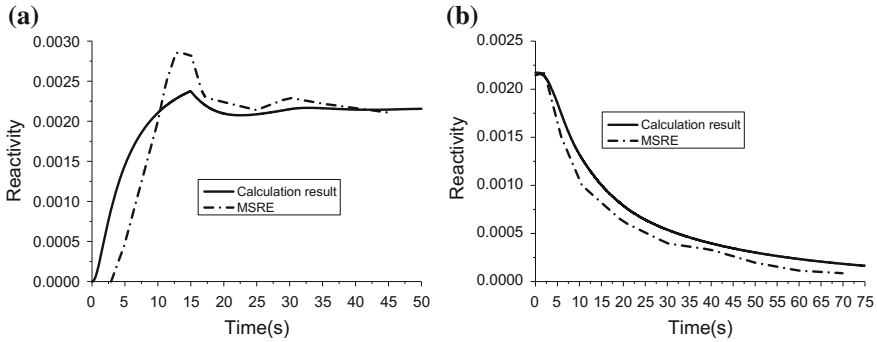


Fig. 2 Reactivity inserted during fuel pump start-up (a) and coast-down (b) transients

delayed neutron precursors flows outside of the core following the fuel salt (Fig. 3a), which leads to reactivity lost. Reactivity will be compensated by withdrawing a control rod, so as to keep reactor critical. As the fuel pump coast down, the portion of delayed neutron precursors flowing outside the core decreases because the fuel speed reduces (Fig. 3b), which results in the reactivity rise. In order to keep reactor power at a constant level, negative reactivity will be inserted in the core by adjusting a control rod.

The comparison of calculation result and experiment data of natural circulation benchmark is shown in Figs. 4 and 5. During the natural circulation transient the fuel pump was turned off. The only source of fuel salt flow rate was natural circulation due to temperature difference between core inlet and outlet. Initially the power of reactor was only 4 kW, flow rate of fuel salt was almost zero with the reactor equilibrium. Transient experiment was driven by gradually increasing the heat removal rate in the heat exchanger, keeping the core critical and waiting for the system to be steady state before the next motion. Increasing heat removal rate in heat exchanger led to the decreasing of temperature at the core inlet, which

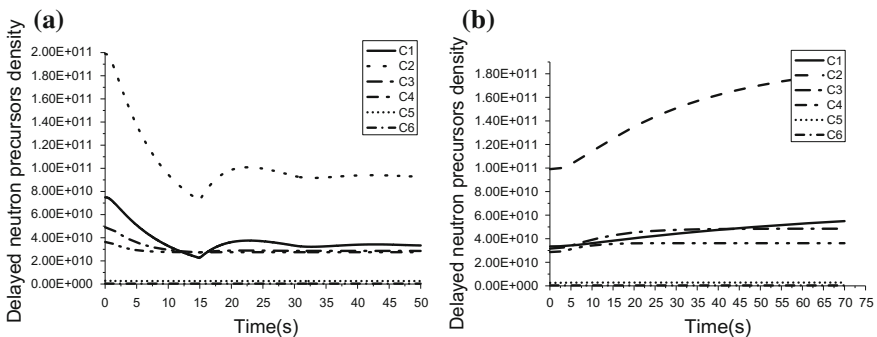


Fig. 3 Density of delayed neutron precursors in the core during fuel pump start-up (a) and coast-down (b) transients

Fig. 4 Reactor power during the nature circulation transient

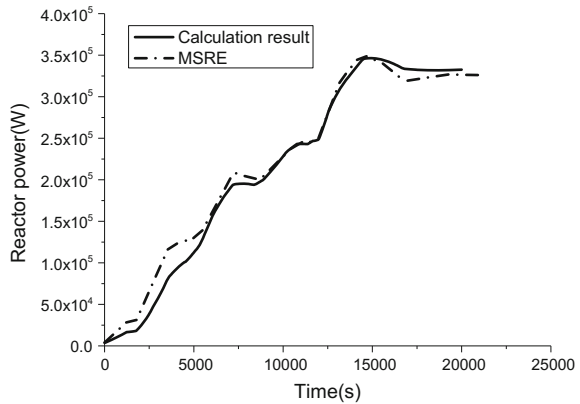
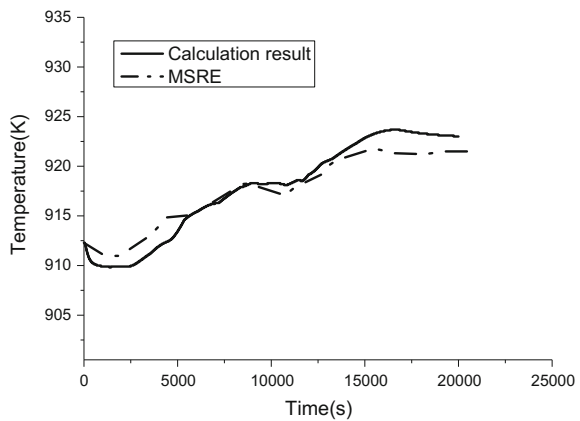


Fig. 5 Core outlet temperature during the natural circulation transient



caused the reactivity rising due to the negative temperature feedback of fuel salt and graphite. This in turn caused the reactor power to increase. Both the decrease of temperature at core inlet and the increase of temperature at core outlet raised the temperature difference between core inlet and outlet, resulting in the higher flow rate of fuel salt due to nature circulation.

The calculation results coincide well with experimental data of three benchmarks above, which verifies the validity of the model and the extended RELAP5 code.

4 Conclusions

Liquid fuel molten salt reactor is special due to its fuel flow effect, so the thermal hydraulic and point kinetic models are different from traditional solid fuel reactor.

Based on the original structure of original RELAP5 code, new thermal hydraulic and point kinetic models for liquid fuel molten salt reactor were added, and the corresponding solving method was extended. Using the MSRE pump start-up, pump coast-down, and natural circulation experiments as the benchmarks, the validity of liquid fuel molten salt reactor models and modified system analysis code were verified. The results indicate that extended RELAP5 code is suitable to the system safety analysis of liquid fuel molten salt reactor system.

References

1. Bettis E.S., Schroeder R.W., Cristy G.A., et al., 1957. The aircraft reactor experiment-design and construction. *Nucl. Sci. Eng.* 2, 804–825
2. Rosenthal M.W., Kasten P.R., Briggs R.B., 1970. Molten-salt reactors-history, states, and potential. *Nucl. Appl. Technol.* 8, 107–117
3. Robertson R.C., 1971. Conceptual design study of a single-fluid molten-salt breeder reactor. Oak Ridge National Laboratory. ORNL-4541
4. Furukawa K., Arakawa K., Erbay L.B., et al., 2008. A road map for the realization of global-scale thorium breeding fuel cycle by single molten-fluoride flow. *Energy Convers. Manag.* 49, 1832–1847
5. Ignatiev V., Afonichkin V., Feynberg O., et al., 2006. Progress in integrated study of molten salt actinide recycler and transmuter system. In: *Proc. Ninth Information Exchange Meeting on Actinide and Fission Product Partitioning and Transmutation*, France, September 25–29, 2006, Nuclear Energy Agency
6. Jiang M., Xu H., Dai Z., 2012. Advanced fission energy Program - TMSR Nuclear Energy System. *Bulletin of the Chinese Academy of Sciences.* 27 (03), 366–374
7. Lecarpentier D., Carpentier V., 2003. A neutronic program for critical and non-equilibrium study of mobile fuel reactors: the Cinsf1D code. *Nucl. Sci. Eng.* 143, 33–46
8. Krepel J., Grundmann U., Rohde U., 2005. DYN1D-MSR dynamics code for molten salt reactors. *Ann. Nucl. Energy.* 32, 1799–1824
9. Krepel J., Grundmann U., Rohde U., 2007. DYN3D-MSR spatial dynamics code for molten salt reactors. *Ann. Nucl. Energy.* 34, 449–462
10. Wang S., Rineiski A., Maschek W., 2006. Molten salt related extensions of the SIMMER-III code and its application for a burner reactor. *Nucl. Eng. Des.* 236, 1580–1588
11. Guo Z., Zhang D., Xiao Y., et al., 2013. Simulations of unprotected loss of heat sink and combination of events accidents for a molten salt reactor. *Ann. Nucl. Energy.* 53, 309–319
12. Hayashi H., 1996. Numerical solution of retarded and neutral delay differential equations using continuous Runger-Kutta methods. Graduate Department of Computer Science, University of Toronto. 13–22
13. Cohen E.R., Hetrick D.L., Homing W.A., 1958. A survey of nuclear reactor kinetics. Second United Nations International Conference on the Peaceful Uses of Atomic Energy, March 7, 1958
14. Prince B.E., Ball S.J., Engel J.R., et al., 1968. Zero-power physics experiments on the molten salt reactor experiment. Oak Ridge National Laboratory. ORNL-4233
15. Rosenthal M.W., Briggs R.B., Kasten P.R., 1969. Molten-salt reactor program semiannual progress report. Oak Ridge National Laboratory. ORNL-4396
16. Robertson R.C., 1965. MSRE Design and Operation Report, Part I, Description of Reactor Design. Oak Ridge National Laboratory. ORNL-TM-728
17. Auwerda G.J., 2007. Computational modeling of a molten salt reactor. TU Delft